Incidence-angle selection and spatial reshaping of terahertz pulses in optical tunneling

M. T. Reiten, K. McClatchey, D. Grischkowsky, and R. A. Cheville

School of Electrical and Computer Engineering and Center for Laser and Photonics Research, Oklahoma State University, Stillwater, Oklahoma 74078

Received July 31, 2001

We present spatially resolved measurements of the electric field of terahertz pulses undergoing optical tunneling that show strong pulse reshaping in both time and space. This reshaping is shown to be a result of frequency and incidence-angle filtering of the complex amplitude of the plane-wave basis set that makes up the pulse. This filtering leads to spreading of the pulse in the time and space dimensions, as expected from linear dispersion theory. Measurement of the pulse shape after transmission through an optical tunneling barrier permits direct determination of the complex system transfer function in two dimensions. The transfer function, measured over both thin and thick barrier limits, contains a complete description of the tunneling barrier system from which the phase and loss times can be directly determined. © 2001 Optical Society of America

OCIS codes: 320.7150, 320.5540, 260.6970, 070.6110.

The question of optical tunneling, originally addressed by Brillouin and Sommerfeld,[1] has received considerable attention in the scientific literature, both historically and currently, specifically in terms of the time scale associated with tunneling phenomena. Since optical tunneling results in pulse reshaping, it is difficult to directly assign a tunneling time for strongly reshaped pulses.[2] Hence, two time scales have been proposed for tunneling[3]: A loss time describes pulse attenuation, and a phase time describes temporal shifts or reshaping.

Here we extend previous investigations[4,5] of optical tunneling with near-single-cycle pulses with extremely broad bandwidths to measure the effect of spatial as well as temporal pulse reshaping. These previous experiments reached opposing conclusions on whether light propagation is causal. Here we show that as temporal pulse reshaping makes it impossible to assign a time to tunneling,[2] similarly, spatial pulse reshaping makes it impossible to assign a well-defined path to spatially localized wave packets. By direct coherent measurement of the pulse's electric field, we directly measure the complex propagation time.

The terahertz (THz) system[6] is similar to that used in previous investigations[5] and is shown schematically in Fig. 1(a). Silicon wedges cut so that the incidence angle, θ, of the terahertz (THz) pulse on the silicon–air interface is past the critical angle are used to create the optical tunneling barrier, which is placed at a waist of the THz beam to ensure a nearly planar phase front. Unlike in the previous investigations, the THz pulse is measured with 1-mm spatial resolution and subpicosecond temporal resolution by a fiber-coupled 50-μm dipole antenna structure that can be translated along the x direction. No collection lens is used on the detection dipole, which permits high spatial resolution, thereby reducing the bandwidth of the THz system. In these investigations the wedge separation along the cylinder axis, Δ, and the angle of the systems's optical axis to the cylinder axis, β, are adjustable with resolutions of less than 5 μm and 0.5°, respectively; only the wedge closest to the paraboloidal mirror was moved to change Δ. The angle between the THz beam's optical axis ($\hat{z}$ axis) and the cylinder axis, β, is 10.0°, so the angle of incidence on the interior wedge face is $\theta = 17.1°$, 0.1° off the critical angle of 17.0°.

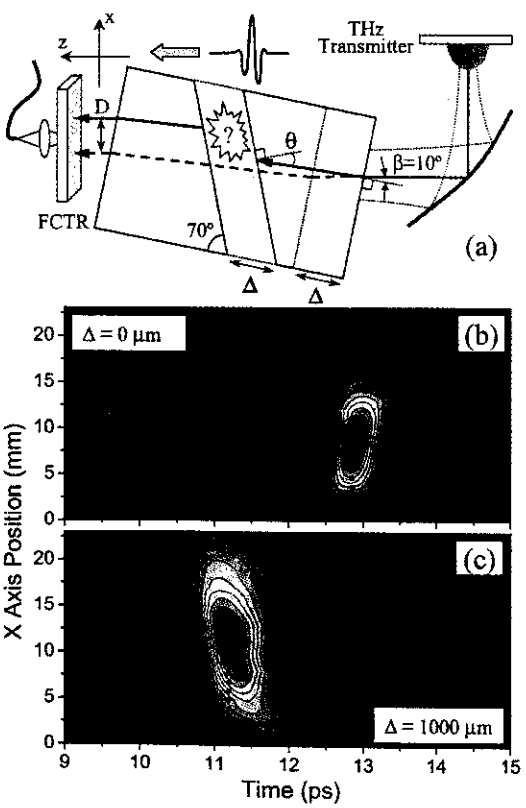

Fig. 1. (a) Experimental schematic of a fiber-coupled THz receiver (FCTR). The lines represent the propagation path (dashed line, $\Delta = 0$ μm; solid line, $\Delta = 1000$ μm). Contour plots: (b) $E_0(x, t)$ with 15-pA contour spacing, (c) $E_T(x, t)$ with 5-pA spacing.

0146-9592/01/231900-03$15.00/0

The time-resolved THz pulse was measured at 26 positions along the x direction spaced 1 mm apart, yielding a two-dimensional slice of the cylindrically symmetric THz beam's electric field as a function of x position and time. Contour plots of the measured electric field amplitude are shown in Fig. 1(b) for the reference pulse, $E_0(x, t)$, with no gap ($\Delta = 0$), and in Fig. 1(c) for the pulse that has tunneled through an optical barrier, $E_T(x, t)$, of width $\Delta = 1000$ μm. The peak of the pulse with $\Delta = 1000$ μm, $E_T(x, t)$, shows a shift of -1.79 ps relative to $E_0(x, t)$, observed previously.[4,5] The peak also shifts a distance $D = 2.8$ mm spatially in the positive x direction, propagating through less high-index material than the reference pulse, opposite to what was assumed in an earlier study that claimed superluminal, noncausal propagation.[4] The tilt of the cylinder axis results in a lateral shift artifact of 152 μm for $\Delta = 1000$ μm, below the spatial resolution of our measurement. The spatial shift is due to the refraction of the plane waves that make up the pulse, incident at various angles. Some of the angles are complex.[5] This shift is analogous to the Goos–Hänchen shift that occurs during total internal reflection of a spatially bounded beam, which is dependent on the spatial and spectral profiles of the THz pulse. The shift at the center frequency of the THz pulse is calculated[7] to be 4.4 mm, in reasonable agreement with the measurement.

Shifting pulse peaks or centroids is not sufficient for rigorous determination of propagation times.[2] Thus, to analyze the propagation of time- and spatially dependent pulses tunneling through an optical barrier, we use linear dispersion theory[5] by expanding the pulse into a superposition of plane waves. The frequency-dependent complex amplitude at a given spatial position, $E(\omega, x)$, is obtained through the Fourier transform of the measured THz pulse, $E(x, t)$. The spatially localized THz beam is composed of a summation of plane waves corresponding to a distribution of incidence angles, each with a given amplitude and phase relationship. The angle of each plane-wave component relative to the beam-propagation axis inside the silicon is[7] $\phi = \arctan(k_x/k_z)$, where k_z is determined by $k_z^2 = k^2 - k_x^2$. Here $k = |\mathbf{k}| = \omega n/c$ for a given frequency, n is the refractive index of silicon, ω is the angular frequency, and c is the speed of light. For our geometry, $\phi \ll 1$, so $\phi \cong k_x/k_z \cong k_x/k$, and the actual angle of incidence on the gap forming the tunneling barrier is $\theta - \phi$, with $\theta = 17.1°$, such that negative values of ϕ correspond to larger incidence angles. The complex amplitude of each plane-wave component of the bounded beam is obtained by a second Fourier transform:

$$E(k_x, \omega_0) = \int_{-\infty}^{\infty} E(r, \omega_0)\exp(-ik_x x)\partial x\,, \qquad (1)$$

where the value of k_x determines the angle of incidence, $\phi \cong k_x c/n\omega$. The two Fourier transforms convert the temporally and spatially localized THz pulse into a basis set of plane waves with propagation vectors in the $\hat{x}\hat{z}$ plane. Although they are not shown, the spatially resolved pulses shown in Figs. 1(b) and 1(c) are measured to have planar phase fronts, as expected from the experimental configuration, in which a beam waist is placed at the optical tunneling barrier with increasing diameter with wavelength.

The relative amplitude of the plane-wave components making up the reference pulse, $|E_0(\phi, \omega)|$, is shown in Fig. 2(a) and was obtained from $E_0(x, t)$ of Fig. 1(b). The ϕ axis assumes a medium of index $n = 3.42$ to illustrate the angular spread of incidence angles of the bounded THz beam incident on the tunneling barrier. There is a small experimental artifact in the measurement of $|E_0(\phi, \omega)|$ that is due to the limited experimental range of 25 mm. The amplitude distribution of the THz pulse with $\Delta = 1000$ μm, $|E_T(\phi, \omega)|$, is shown in Fig. 2(b). The peak spectral component of $|E_T(\phi, \omega)|$ has shifted from 0.32 to 0.21 THz because of the decay of the evanescent waves within the gap with a characteristic amplitude attenuation length, L, proportional to wavelength.[5] In addition to spectral reshaping along the ω axis in Fig. 2(b), the amplitude spectrum also is reshaped along the ϕ axis. Physically the broadening is due to the rapid change of L as the incident plane waves exceed the critical angle. This changing L results in a change in propagation direction for the pulse propagated through the barrier as observed previously at optical frequencies[8] and also in the spatial broadening that can be seen in Figs. 1(b) and 1(c).

Although the barrier-traversal time cannot be determined directly from pulse measurements,[2] the

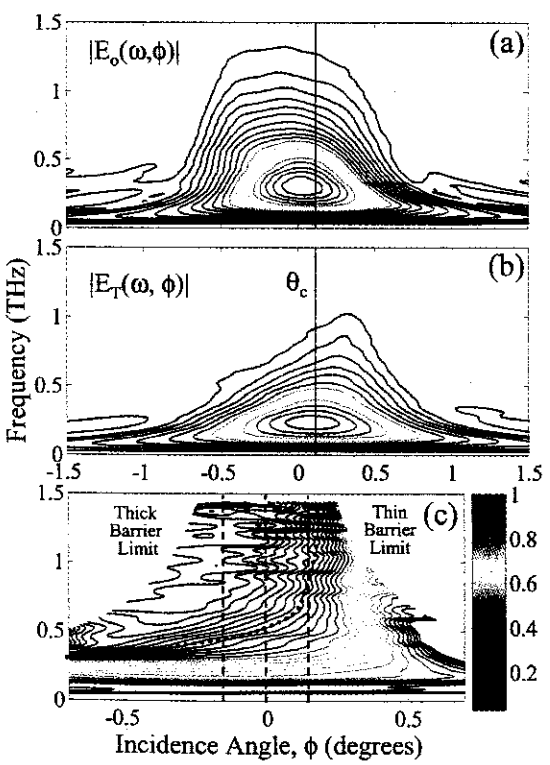

Fig. 2. (a) Normalized $|E_0(\phi, \omega)|$, $\Delta = 0$ μm. (b) $|E_T(\phi, \omega)|$, $\Delta = 1000$ μm normalized to $|E_0(\phi, \omega)|$. The contour line spacing is 0.05, and the vertical line is θ_c. (c) $|H(\phi, \omega)|$. The dashed lines are constant ϕ values of Fig. 3, and the dotted curve represents the thick–thin barrier boundary.

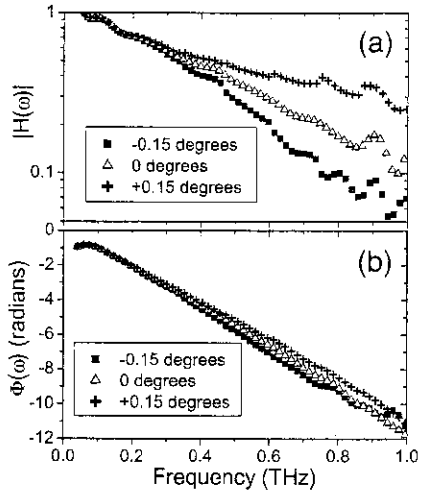

Fig. 3. (a) Semilog plot of $|H(\phi, \omega)|$ and (b) linear plot of $\Phi(\phi, \omega)$ for $\phi = -0.15°, 0°, +0.15°$.

transfer function contains a complete description of pulse propagation through the wedge–gap system as a whole.[5] This description permits direct determination of the propagation time through the system for each plane-wave component. The experimentally measured complex transfer function, $H(\phi, \omega)$, is

$$\frac{E_T(\phi, \omega)}{E_0(\phi, \omega)} = H(\phi, \omega) = |H(\phi, \omega)| \exp[i\Phi(\phi, \omega)]. \quad (2)$$

The complex transfer function, $H(\phi, \omega)$, is determined over both the thick ($\Delta \gg L$) and the thin ($\Delta \ll L$) barrier limits, and the magnitude is shown in Fig. 2(c). The dotted curve is a guide for the eye.

The complex traversal time, $\tau_c = \tau_\Phi + i\tau_L$, is determined from $H(\phi, \omega)$ and describes propagation of the THz pulse through the wedge–gap system.[8] The complex traversal time is given by the phase time, τ_Φ, and a loss time, τ_L. The phase time corresponds to the group velocity, and the interpretation of the loss time shift that is due to the pulse reshaping[3]:

$$\tau_\Phi = \frac{\partial \Phi}{\partial \omega}, \qquad \tau_L = -\frac{\partial \ln|H(\phi, \omega)|}{\partial \omega}. \quad (3)$$

The amplitudes and phase relationships of $H(\phi, \omega)$ as a function of frequency for three values of ϕ, corresponding to the dashed lines in Fig. 2(c), are shown in Fig. 3. The magnitude of the measured transfer function, Fig. 3(a), falls exponentially with increasing frequency and depends strongly on ϕ. The slopes directly yield loss times τ_L of 1.4, 2.4, and 3.4 ps for $\phi = -0.15°$, $\phi = 0°$, and $\phi = +0.15°$, respectively. $H(\omega)$ shows a linear phase shift between the signal and reference pulses [Fig. 3(b)], with a negative slope corresponding to a shift forward in time, as observed in Fig. 1. The slopes give the phase times of the system, $\tau_\Phi = -1.25, -1.18, -1.06 (\pm 0.15$ ps) for $\phi = -0.15°, 0°, +0.15°$. The phase times are of the same order as the measured peak shift of -1.79 ps. These loss and phase times are analogous to those measured previously by measurement of beam-angle divergence with cw optical frequencies[8] but are determined directly from phase-coherent data over a broad spectral range. For the value of $\Delta = 1000$ μm and the frequency spectrum measured here, we do not observe saturation of the phase times.[8]

The authors acknowledge the support of the National Science Foundation (NSF) and the Army Research Office. K. McClatchey acknowledges the support of the NSF Research Experience for Undergraduates program. R. A. Cheville's e-mail address is kridnix@thzsun.ecen.okstate.edu.

References

1. L. Brillouin, *Wave Propagation and Group Velocity* (Academic, New York, 1960).
2. R. Landauer and Th. Martin, "Barrier interaction time in tunneling," Rev. Mod. Phys. **66,** 217–221 (1994).
3. R. Y. Chiao and A. M. Steinberg, "Tunneling times and superluminality," in *Progress in Optics*, E. Wolf, ed. (Elsevier, Amsterdam, 1997), Vol. 37 pp. 345–405.
4. J. J. Carey, J. Zawadzka, D. A. Jaroszynski, and K. Wynne, "Noncausal time response in frustrated total internal reflection," Phys. Rev. Lett. **84,** 1431–1434 (2000).
5. M. T. Reiten, D. Grischkowsky, and R. A. Cheville, Phys. Rev. E **64,** 036604 (2001).
6. D. Grischkowsky, S. Keiding, M. van Exter, and Ch. Fattinger, "Far-infrared time-domain spectroscopy with terahertz beams of dielectrics and semiconductors," J. Opt. Soc. Am. B **7,** 2006–2015 (1990).
7. A. K. Ghatak, M. R. Shenoy, I. C. Goyal, and K. Thyagarajan, "Beam propagation under frustrated total internal reflection," Opt. Commun. **56,** 313–317 (1986).
8. Ph. Balcou and L. Dutriaux, "Dual optical tunneling times is frustrated total internal reflection," Phys. Rev. Lett. **78,** 851–854 (1997).